Synthesis and Electrochemical Studies of New Antimalarial Endoperoxides

Fadia Najjar,[a] Michel Baltas,[a] Liliane Gorrichon,[a] Yolande Moreno,[a] Theodore Tzedakis,[b] Henri Vial,[c] and Christiane André-Barrès*[a]

Keywords: Biological activity / Electrochemistry / Natural products / Peroxides

Structural analogues of endoperoxides belonging to the family of G factors have been synthesized under Mannich-type conditions. The structures of the different diastereoisomers have been established from NMR spectroscopic data. Their cathodic peak potentials have been determined by thin layer electrochemistry under potentiostatic conditions, and compared to artemisinin. These endoperoxides were evaluated in vitro against *Plasmodium falciparum* and showed moderate to good activity.

Introduction

Endoperoxides are important chemical frameworks in the activity of a number of pharmacologically active compounds. Examples include the natural products chondrillin (**1**) and analogues, which show significant antitumor activity,[1] artemisinin (qinghaosu, **2**;[2] Figure 1) and yingzhaosu (**3**),[3] both isolated from traditional Chinese herbal treatments, which are potent antimalarial compounds.

Malaria is a disease caused by parasitic protozoa belonging to the Plasmodium genus, mostly *Plasmodium falciparum*. This disease affects some 200−300 million people worldwide every year. The anti-malarial properties of non-alkaloid compounds such as artemisinin **2** and its related endoperoxides **3** have attracted considerable attention and these compounds are widely used, as they are one of the few effective treatments for multi-drug resistant *P. falciparum* malaria. These compounds are active against the early form of the malarial blood stages and induce rapid clearance of blood parasitemia, and no resistance has been confirmed. Nevertheless, since malaria parasites are rapidly developing drug resistance, there is an increasing need for more accessible and more effective drugs. To that goal, a number of derivatives possessing the endoperoxide framework have been designed and synthesized, including arteflene (**4**),[4] a synthetic derivative of yingzhaosu (**3**),[5] BO7 (**5**),[6] a *cis*-fused cyclopenteno 1,2,4-trioxane, or the cyclic peroxyketals **6** prepared by Posner.[7] The molecule 1,2,4,5-tetraoxane **7** (WR148999), although quite different from **2**, also displays antimalarial activity. Recently, B. Meunier described synthesis of "trioxaquines"[8] **8**, hybrid compounds with both trioxane and 4-aminoquinoline moieties. In all of those compounds exhibiting good activity (in the nanomolar range) on chloroquine-resistant *Plasmodium* strains, the endoperoxide framework seems to be vital for the activity to occur.

The key steps in the mechanism of antimalarial endoperoxide action are contact with haeme iron and electron transfer (ET) resulting in the cleavage of the O−O bond. Oxygen-centered radical intermediates are formed first, and then carbon-centered radicals, high valent iron, and other reactive intermediates. All these species may then interact with so far unidentified vital intercellular target molecules, through undefined mechanisms, resulting in the death of the parasite. The cleavage process has been intensively investigated in various model systems with haeme or non-haeme iron.[8]

The naturally occurring G factors (G1, G2, G3) constitute a family of six-membered unsaturated cyclic endoperoxides fused to another six-carbon ring deriving from syncarpic acid. The G factors were first isolated from *Eucalyptus grandis.* They act as phytohormones and seem to be involved in frost resistance and water loss reduction in these species. They cannot be present in their physiological forms, but rather in some inactive form, and are readily released in response to damage to the plant or to a biological stimulus.[9]

In this paper we report the synthesis of G factor analogues **13**−**15**, by a previously developed method,[10] and of

[a] Synthèse et Physicochimie de Molécules d'Intérêt Biologique, UMR CNRS 5068, Université Paul Sabatier,
118 route de Narbonne, 31062 Toulouse cedex 04, France
Fax: (internat.) + 33-5/61558255
E-mail: candre@chimie.ups-tlse.fr
[b] Laboratoire du Génie Chimique, UMR CNRS 5503, Université Paul Sabatier,
118 route de Narbonne, 31062 Toulouse cedex 04, France
[c] Dynamique Moléculaires des Interactions Membranaires, UMR CNRS 5539, Université Montpellier 2,
cc107, Place E. Bataillon, 34095 Montpellier Cedex 5, France

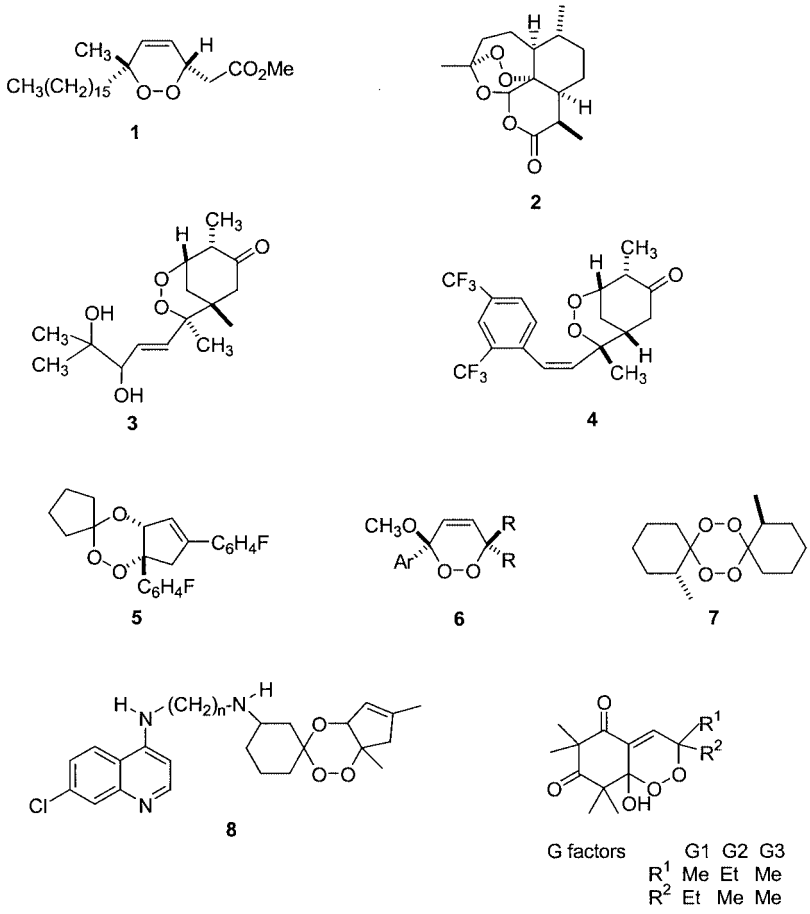

Figure 1. Some examples of biologically active endoperoxides

their methylated derivatives **16**−**18**, together with the determination of their reduction potentials and evaluation of their biological activity. Tertiary hydroxy methylated compounds were synthesized for two reasons: firstly, from analogy to Posner's antimalarial cyclic peroxyketals,[6] which showed that antimalarial activity is higher when the hemiketal position is methylated, lower when OH is free and decreases when OH is alkylated by a too hindered isopropyl group, and secondly, in order to evaluate the effect of the methyl group in mimicking the trioxane structure of artemisinin.

In view of the possible mode of action of these compounds, proper consideration of the role of electron transfer (ET) in systems possessing a peroxide linkage involved in their biological activity requires knowledge of the reduction potentials of the endoperoxides.[11]

Finally, biological results concerning the activity of the synthesised peroxides against the human malarial parasite *Plasmodium falciparum* are discussed.

Results and Discussion

The synthesis of the target compounds was undertaken under Mannich-type conditions.[10] Mannich bases were formed from reactions between syncarpic acid **9** and aldehydes **10**, **11**, and **12**, in the presence of stoichiometric amounts of piperidine (Scheme 1). These Mannich bases could be isolated in high yield and are stabilised by internal hydrogen bonding. In aqueous acid, rapid piperidine elimination occurs and the ene-one (in equilibrium with dieneol) system spontaneously adds oxygen to give the endoperoxide structure. The speed of oxygen uptake is dependent on the substituents.

The starting aldehydes for the endoperoxides **13** and **14** are commercially available, while for endoperoxide **15**, 2-methyl-3-[(*tert*-butyldiphenylsilyl)oxy]propanal (**12**) was synthesised from 2-methyl-1,3-propanediol in two steps [monoprotection followed by Doëring oxidation ($Pyr{\cdot}SO_3$, DMSO, Et_3N, CH_2Cl_2)] in 75% overall yield.

For (±)-2-phenylpropionaldehyde (**11**), two diastereomeric products **14a** and **14b** were obtained in an overall yield of 70% (60:40), and could be separated by chromatography. The structure of each isomer was attributed with the aid of NMR HSQC (Heteronuclear Single Quantum Coherence) ^1H-^{13}C COSY spectra followed by HMBC (Heteronuclear Multiple Bond Connectivity), giving complete assignments of both ^1H and ^{13}C spectra. The relative stereochemistry of each isomer and differentiation between methyl groups in each *gem*-dimethyl frame was determined

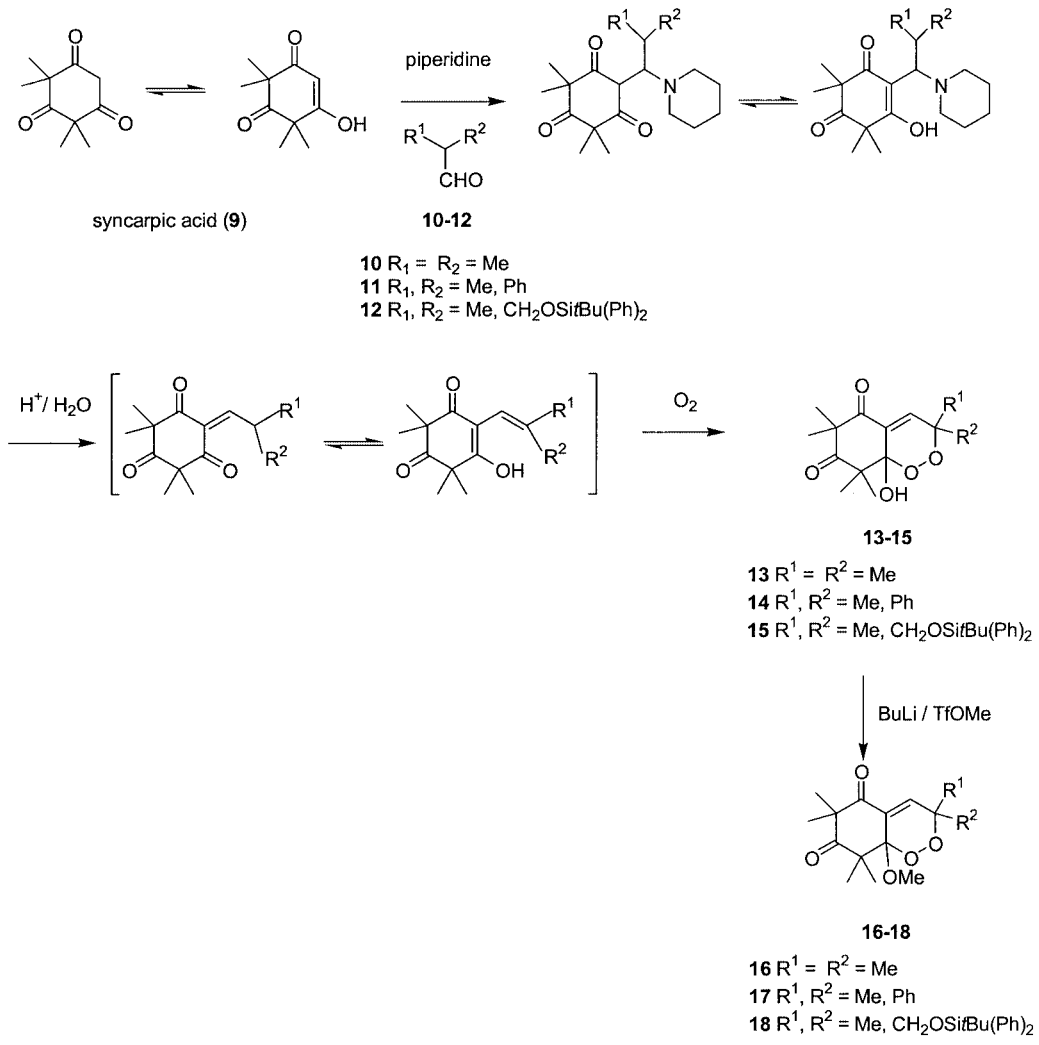

Scheme 1. Synthesis of endoperoxides **13**−**15** and methylated compounds **16**−**18**

by NOESY spectroscopy. Diastereoisomer **14b** was assigned as the one displaying NOE effects (Figure 2) between the C15 methyl group and each C11 and C13 methyl, while no effect was observed for diastereoisomer **14a**. In this latter case, a *trans* relationship between the OH and Ph groups was observed.

Treatment of aldehyde (±)-**12** with syncarpic acid gave, after removal of the amine, a complex mixture that evolved slowly. After eight days, endoperoxides **15a** and **15b** were isolated from the crude mixture in 60% yield (75:25) by silica gel chromatography (Table 1).

Similar experiments were undertaken in order to establish the relative stereochemistry of endoperoxides **15a** and **15b**. HSQC, HMBC, and NOESY experiments confirmed the same *trans* relationship between OH and $CH_2OSi(Ph)_2tBu$ for compound **15a**, and *cis* for compound **15b**.

Modelling studies were performed on compounds **14a**, **14b**, **15a**, and **15b**. The optimal conformations obtained through energy minimization[12] showed spatial proximity between the C11 and C15 methyl groups for **14b** (Figure 3), in agreement with the observed NOE effect. Similar results observed for compounds **15a** and **15b** suggested the same conclusions.

Methylation of the tertiary hydroxyl group was undertaken. Although this reaction is reported to be efficient in acidic medium (H^+/methanol) for other peroxides possessing an adjacent tertiary hydroxyl group[13] it was unsuccessful in the present case. Endoperoxide **13** could not be derivatised but rather underwent degradation. Methyl iodide was found to be inert under basic conditions (*n*BuLi, MeI). Gratifyingly though, under basic conditions[14] endoperoxide **13** reacted well with methyl triflate to produce the methylated compound **16** in 70% yield. The same methodology (BuLi/TfOMe) was used to methylate **14a**, **14b**, **15a**, and **15b**. All of these reactions afforded methylated compounds − **17a**, **17b**, **18a**, and **18b**, respectively − in good yields (about 70%). NMR HSQC, HMBC, and NOESY experiments were undertaken on the methylated series and confirmed the stereochemistry. **NOE** effects are observed between OMe and the C15 methyl group for compounds

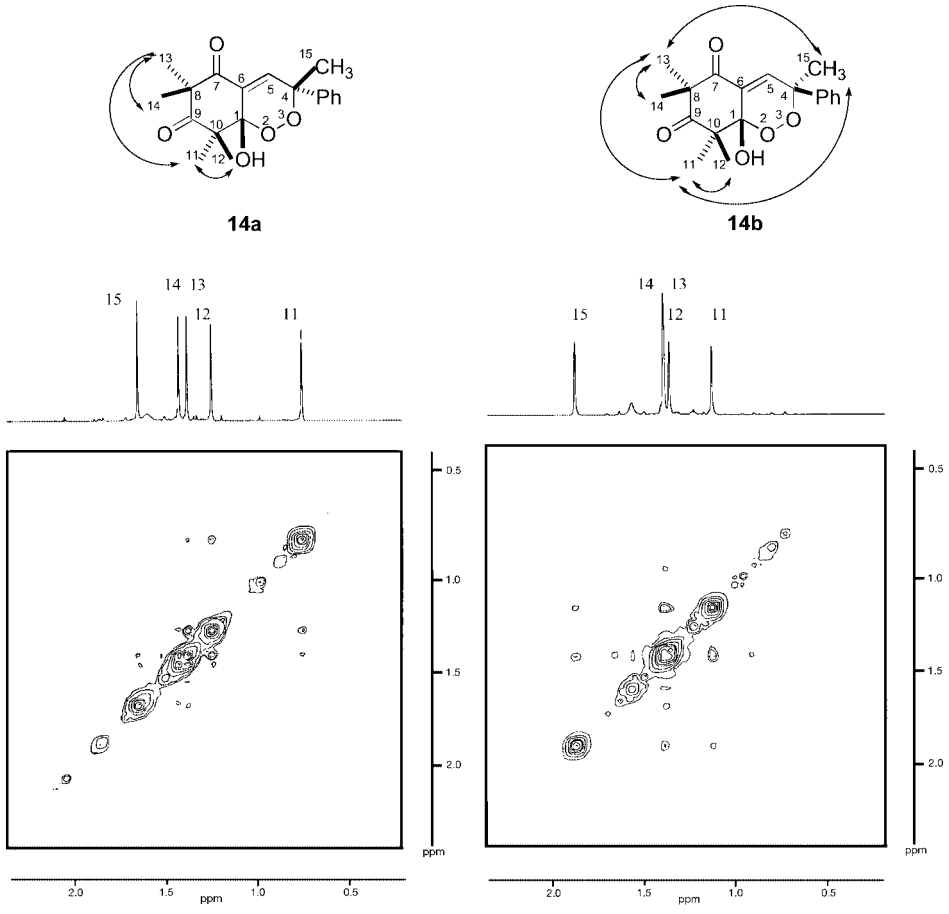

Figure 2. NOESY experiments for compounds **14a** and **14b**

Table 1. Yields in the synthesis of endoperoxides issued from syncarpic acid

Endoperoxides	R^1	R^2	Yield *(diastereomeric ratio)*
13	Me	Me	85%
14a	Me	Ph	70% *(60:40)*
14b	Ph	Me	
15a	Me	$CH_2OSi(Ph)_2tBu$	60% *(75:25)*
15b	$CH_2OSi(Ph)_2tBu$	Me	

17a and **18a**, but not for **17b** and **18b**. Typical NOESY experiments are shown for compounds **18a** and **18b** in Figure 4.

Electrochemical Studies

For consideration of the role of electron transfer in the possible mode of action of cyclic endoperoxides, accurate values for their reduction potentials are required. The electrochemical behaviour of endoperoxides **13**−**18** was studied and compared with that of artemisinin, by use of a thin layer voltammetry method under potentiostatic conditions. The method used is an original way to determine anodic peak potentials (E_p) on small quantities and to obtain a relative and comparative scale between these compounds and artemisinin in the reduction step of the endoperoxide function.

Carbon felt (COMAIP France; reference CFT 3000 10), set between two glass slides delimiting a compartment with a volume of a few tens of μL, was used as working electrode. The choice of carbon was justified by the high cathodic overvoltage in DMF solvent (ca. 2 V). Because of the small volume of the thin-layer cell, all the electroactive molecules present in solution can be transformed during one scan. There is no mixing between the solution of the thin layer cell and the solution of the auxiliary electrode compartment, so it is possible to examine the behaviour of products appearing at the electrode during the potential scan. From the amount of charge, determination of the number of electrons exchanged during the electrode reaction is straightforward.

All the electrode potentials were measured with respect to a saturated calomel electrode (SCE; $Hg/Hg_2Cl_2/Cl^-$ satu-

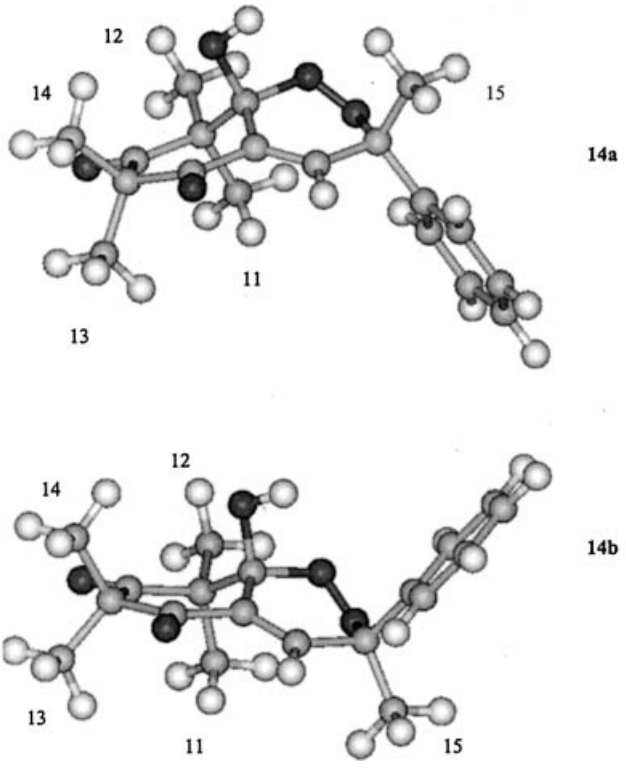

Figure 3. Energetically optimal conformations through modelling studies of compounds **14a** and **14b**

rated), immersed in a Luggin capillary located close to (3−4 mm) the working electrode and containing DMF and the electrolyte in large excess. The auxiliary electrode was made of platinum. The electrochemical apparatus used was a Radiometer Voltalab PGZ 100 computerised potentiostat. The electrochemical cell was kept under an inert atmosphere (nitrogen at 1.5 atm) and all experiments were performed in the absence of oxygen.

Current-potential curves were typically obtained with endoperoxides at a 0.01 M concentration with use of 0.3 mol·L^{-1} of $NEt_4^+ClO_4^-$ as electrolyte in DMF solvent, and are shown in Figure 5.

Table 2 shows the potential of various signals at the cathodic part (first scan). For all compounds (scan rate r = 0.5 mV·s^{-1}), an intense cathodic signal appeared in the −1.4 to −1.8 V range. Integration of the peak showed one electron exchange, suggesting that a radical anion appears at the electrode[15] according to the equation:

$$AB + e^- \rightarrow A^\circ + B^-$$

It is also noteworthy that, for every compound studied, a strong shift between the zero current potential (−0.1 to −0.2 V) and the potential of the peak of reduction of the endoperoxide (−1.4 to −1.8 V) was observed, indicating the presence of slow redox systems (Table 2).

The inversion of the potential scan rate after the end of the cathodic plotting for each endoperoxide was also recorded (Figure 5). It showed that there is no anodic signal in the potential range from −1.7 to −1.2 V, in accordance with the presence of slow redox systems. Several signals are located at potentials higher than ca. −0.8 V, indicating that the reduction of the endoperoxide produces several by-products, the oxidation of which is observed.

Supplementary reverse scanning provided cathodic curves not including any signals in the range from −1.3 to −1.8 V; the absence of endoperoxide indicates the irreversi-

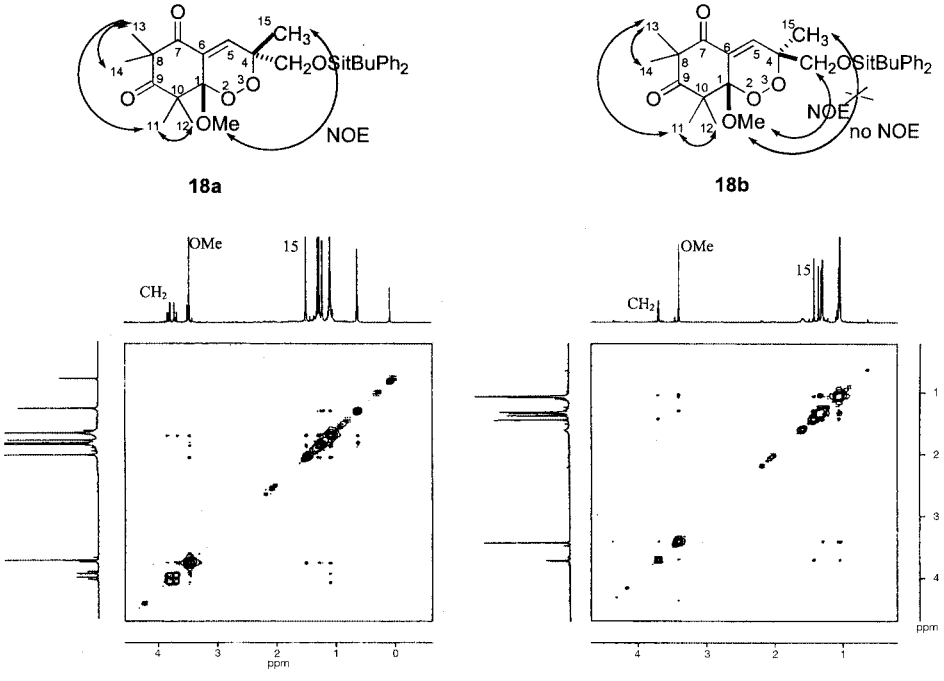

Figure 4. NOESY experiments for compounds **18a** and **18b**

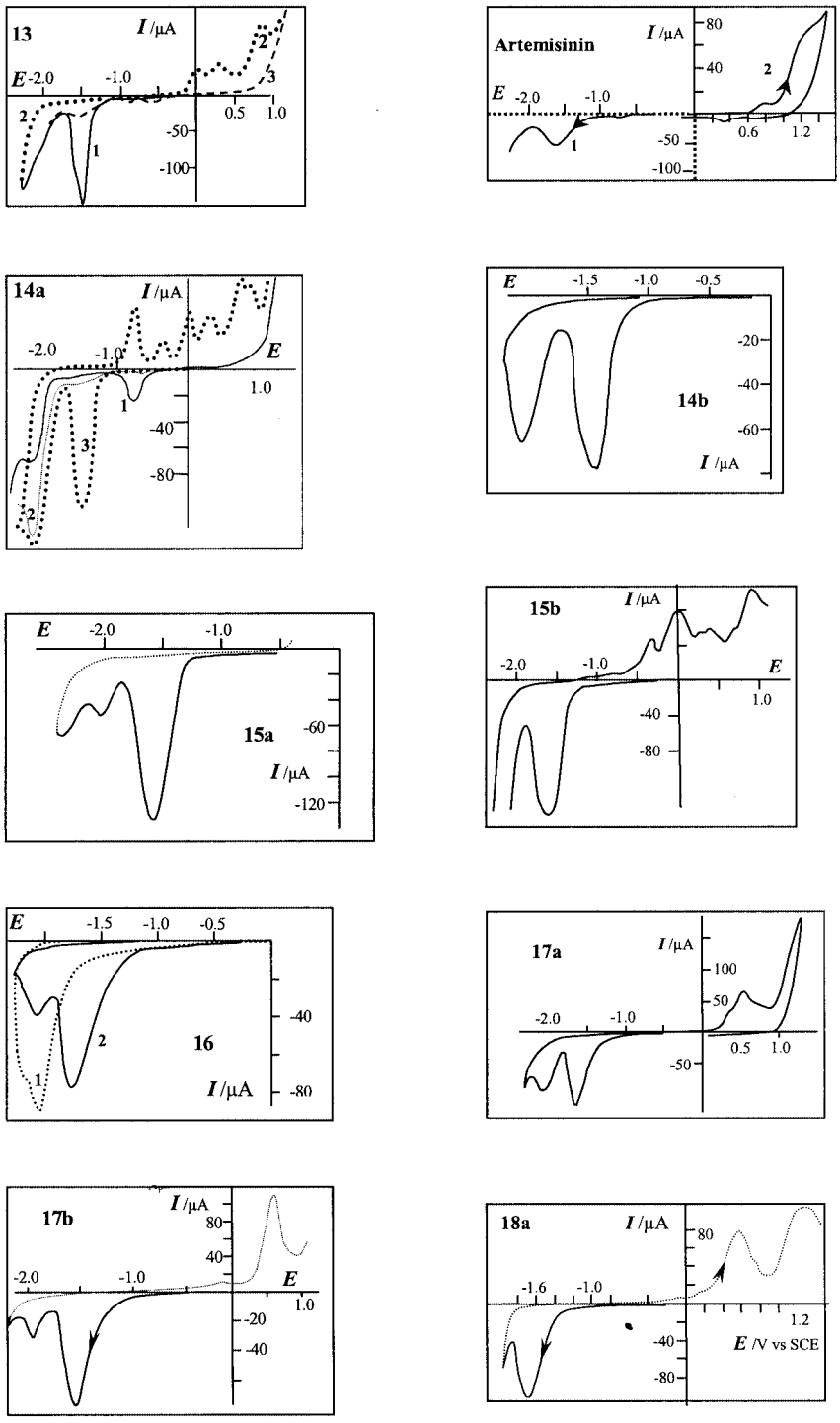

Figure 5. Current-potential curves obtained with carbon felt enclosed in a thin layer cell with various endoperoxides at a concentration of 0.01 M in 0.3 M $NEt_4^+ClO_4^-$ in DMF; temp. ca. 20 °C; r = 0.5 mV·s^{-1}; plotted under 1.5 atm of N_2 unless otherwise indicated. **Artemisin** cathodic (1: V_{TL}: 52 µL) and anodic parts (2: V_{TL}: 54 µL); curves obtained separately; **13**: V_{TL}: 50 µL; plotted order 1, 2, 3. **14a**: 1: residual anodic and cathodic curve, plotted separately in atmospheric air; V_{TL}: 47 µL; 2: residual cathodic curve; V_{TL}: 49 µL; 3: V_{TL}: 51 µL. **14b:** V_{TL}: 37µL. **15a:** V_{TL}: 58 µL. **15b:** V_{TL}: 70 µL. **16**: 1: Residual cathodic curve; V_{TL}: 39µL; 2: V_{TL}: 39 µL. **17a:** V_{TL}: 57 µL. **17b:** V_{TL}: 48 µL. **18a:** V_{TL}: 59 µL

bility of the reduction process under these experimental conditions.

The electrochemical results showed that the E_p values of methylated endoperoxides (**16**−**18b**) are lower than those of the hydroxylated molecules (**13**−**15b**). Some compounds (**16**, **17a**, **18b**) presented redox potentials similar to that of artemisinin, while for the others, the peroxide linkage was easily cleaved. The E_p value of artemisinin found by thin layer voltammetry in our study is similar to that obtained by Workentin.[11] Nevertheless, we have to specify that com-

Table 2. Potentials of the peaks of the various endoperoxides **13**−**18b**, measured on curves obtained by use of an electrochemical thin layer cell and carbon felt as working electrode; all experimental conditions are as indicated in the caption for Figure 5

Endoperoxides	E_p /V vs. SCE (±10 mV) (cathodic part: first scan)
Artemisin	−1.68
13	−1.50
14a	−1.49; −2.16 (solvent)
14b	−1.45
15a	−1.60
15b	−1.52
16	−1.76; −2.06 (solvent)
17a	−1.68; −2.09 (solvent)
17b	−1.55
18a	−1.70
18b	not performed

Table 3. In vitro antimalarial activity of endoperoxides

Endoperoxides	IC_{50} (μM)[a]
Chloroquine	0.030
13	20±10
14a	20±10
14b	27±3
15a	0.7±0.2
15b	0.44±0.06
16	0.28±0.14
17a	2.0±1.0
17b	0.7±0.3
18a	1.5±0.5
18b	1.4±0.4

[a] IC_{50} values were considered acceptable when values did not vary by more than a factor of three.

parison between E_p values can be only qualitative and some discrepancies in E_p values can be noted in the literature,[11,16] indicating the influence of the operating conditions used for the E_p determination in irreversible systems (technique, scan rate, solvent, electrolyte). It is also noteworthy that in irreversible systems the potential of the peaks can be overrated from the corresponding standard potential $E°$. In fact, Workentin[11] showed that artemisinin undergoes an irreversible dissociative reduction by cyclic voltammetry with an anodic peak potential (E_p) that varies with scan rate, being −1.68 V vs. SCE at 1 V/s. The standard potential $E°$ of artemisinin was also determined by these authors, for the first time, as −0.89 V vs. SCE in DMF, so direct electrochemical reduction of artemisinin is subject to a large activation overpotential. Consequently, a rigorous comparison requires knowledge of the standard potential $E°$ of the dissociative reduction of these compounds, the determination of which is the object of an ongoing study.

Biological Studies

The compounds were tested in vitro against the Nigerian strain of *P. falciparum*. All of them exerted potent inhibition on the growth of this human parasite. Inhibition was complete and occurred in a narrow range of concentrations, covering less than two on a log-scale of concentration. The IC_{50} values reported in Table 3 indicate drug concentrations reducing cell growth by up to 50% of that of untreated control after one cycle. They are in the range of 0.2 to 30 μM. Compounds with high lipophilicity were the most active. The activity of the methylated analogues **16**, **17a**, and **17b** was enhanced by an order of ten in relation to compounds **13**, **14a**, and **14b**. Methylation of the tertiary hydroxyl group of the quite lipophilic compounds **15a** and **15b** gave compounds (**18a** and **18b**) with similar activities.

Conclusion

We have synthesised a number of new endoperoxides possessing a peroxyhemiketal or peroxyketal framework and belonging to the family of G factors. The synthesis is easy and modulable and gives an original route to the endoperoxide bridge; it was developed using syncarpic acid obtained by synthesis, although this is a natural product that can also be extracted from *Myrtaceae*. The formation of the peroxide bridge is biomimetic and occurs through spontaneous oxygen uptake by precursors without any sensitizer, under mild conditions and whatever the substituent. This step is very clean, with good yields and no by-products. This class of compounds possesses electrochemical properties approaching those of artemisinin, and clear antimalarial activity over quite a large range of concentrations, from 0.2 to 30 μM. Lipophilicity appears to be another relevant parameter besides redox ability for antimalarial activity in this series. In view of the urgent need for novel classes of antimalarials, and the potential of endoperoxide-based ones, this series of low-molecular-weight compounds could be of interest for the future, especially if structural modifications on substituents R^1 and R^2 were able to improve the antimalarial activity.

Experimental Section

General Remarks: The solvents were dried by standard procedures, distilled, and stored under argon until used. THF and Et_2O were freshly distilled on sodium/benzophenone. CH_2Cl_2 was distilled from CaH_2; DMF was dried and distilled from CaH_2. Commercially available aldehydes were used after purification. Artemisinin was obtained from Aldrich and used as received. All reactions were monitored by thin-layer chromatography (TLC) carried out on aluminium-backed 0.2 mm silica gel 60 plates with fluorescent indicator UV_{254} and/or by developing the plate with a solution of phosphomolybdic acid. HPLC chromatography was carried out on a Jobin−Yvon apparatus on Merck 15μm or Amicon silica (6−35 μm). NMR spectra were recorded at 250 MHz and 400 MHz for ^1H and 62.8 MHz and 100.6 MHz for ^{13}C in $CDCl_3$ solutions with TMS as internal reference. Mass spectra were obtained on a Nermag R10−10 mass spectrometer. Elemental analyses were performed at the Ecole Nationale Supérieure de Chimie de Toulouse.

1-Hydroxy-4,8,8,10,10-pentamethyl-4-phenyl-2,3-dioxabicyclo-[4.4.0]dec-5-ene-7,9-dione (14): A solution of syncarpic acid (**9**,

0.198 g, 1.09 mmol) and piperidine (0.092 g, 1.09 mmol) in dichloromethane (10 mL) was added at 25 °C to a stirred solution of 2-methylpropanal (**10**, 0.148 g, 1.09 mmol) and piperidine (0.046 g, 0.545 mmol) in dichloromethane (10 mL). After 40 min of stirring, all volatile materials were removed under reduced pressure. The solid residue was dissolved in dichloromethane and agitated vigorously with an aqueous solution of 1 M HCl /NH_4Cl (saturated) for 10 min. The organic layer was then separated and dried ($MgSO_4$), and the solvents were evaporated under reduced pressure. The yield of the residual product was nearly quantitative. It was then dissolved in dry chloroform and left for 3 days under air. Evaporation of solvent gave a solid (mixture of **14a** and **14b**), which was purified by HPLC (eluent petroleum ether/CH_2Cl_2/ethyl acetate, 60:32:8), yielding **14a and 14b** (70%; 60:40).

1-Hydroxy-4,8,8,10,10-pentamethyl-4-phenyl-2,3-dioxabicyclo-[4.4.0]dec-5-ene-7,9-dione (14a): White powder; M.p. 160−162 °C. ^{1}H NMR (250 MHz, $CDCl_3$): δ = 7.67 (s, 1 H, C=C*H*), 7.34 (m, 5 H, Ar), 3.80 (s, O*H*), 1.64 (s, 3 H, CH_3 in position 15), 1.41 (s, 3 H, CH_3 in position 14), 1.37 (s, 3 H, CH_3 in position 13), 1.24 (s, 3 H, CH_3 in position 12), 0.74 (s, 3 H, CH_3 in position 11) ppm. ^{13}C NMR (50 MHz, $CDCl_3$): δ = 210.7 (C9), 198.6 (C7), 141.6 (C5), 141.4, 128.6, 128.1, 125.6 (Ar); 132.4 (C6), 97.5 (C1), 82.3 (C4), 55.0 (C8), 51.9 (C10), 26.7 (C14), 26.2 (C15), 24.3 (C13), 20.6 (C11), 15.0 (C12) ppm. MS (DCI/NH_3): *m*/*z* (%) = 348 [MNH_4^+] (45), 365 (12), 269 (100), 304 (95), 313 (39). $C_{19}H_{22}O_5$ (330.4): calcd. C 69.07, H 6.71; found C 69.10, H 6.12.

1-Hydroxy-4,8,8,10,10-pentamethyl-4-phenyl-2,3-dioxabicyclo-[4.4.0]dec-5-ene-7,9-dione (14b): White powder; M.p. 159−160 °C. ^{1}H NMR (250 MHz, $CDCl_3$): δ = 7.46 (s, 1 H, C=C*H*), 7.40 (m, 5 H, Ar), 3.70 (s, O*H*), 1.87 (s, 3 H, CH_3 in position 15), 1.39 (s, 6 H, CH_3 in position 13−14), 1.36 (s, 3 H, CH_3 in position 12), 1.13 (s, 3 H, CH_3 in position 11) ppm. ^{13}C NMR (50 MHz, $CDCl_3$): δ = 210.6 (C9), 198.1 (C7), 141.9 (C5), 137.7, 129.4, 129.0, 126.4 (Ar), 131.5 (C6), 97.6 (C1), 82.6 (C4), 55.1 (C8), 51.9 (C10), 26.6, 24.0 (C13, C14), 23.3 (C15), 21.0 (C11), 15.1 (C12) ppm. MS (DCI/NH_3): *m*/*z* (%) = 348 [MNH_4^+] (4), 330 [M] (4), 299 (100). $C_{19}H_{22}O_5$ (330.4): calcd. C 69.07, H 6.71; found C 69.27, H 6.49.

4-(*tert*-Butyldiphenylsilyloxymethyl)-1-hydroxy-4,8,8,10,10-pentamethyl-2,3-dioxabicyclo[4.4.0]dec-5-ene-7,9-dione (15): A solution of syncarpic acid (**9**, 0.198 g, 1.09 mmol) and piperidine (0.046 g, 0.545 mmol) in dichloromethane (10 mL) was added to a solution of aldehyde **12** (0.356 g, 1.09 mmol) and piperidine (0.92 g, 1.09 mmol) in dichloromethane (10 mL). By the workup described above, we obtained **15a** and **15b** (60%; 75:25) after purification (eluent petroleum ether/diethyl ether, 7:3).

Compound 15a: White powder; M.p. 157 °C. ^{1}H NMR (250 MHz, $CDCl_3$): δ = 7.76−7.58 (m, 4 H, Ar), 7.44−7.28 (m, 6 H, Ar), 7.22 (s, 1 H, C=C*H*), 3.84, 3.73 (2 H, AB system J_{AB} = 10.2 Hz, CH_2-O-Si), 3.56 (s, 1 H, O*H*), 1.50 {s, 3 H, CH-CH_3[$CH_2OSi(Ph)_2$]}, 1.35, 1.33, 1.24, 0.67 (4s, 12 H, 4 × CH_3), 1.09 [s, 9 H, C-(CH_3)$_3$] ppm. ^{13}C NMR (50.28 MHz, $CDCl_3$): δ = 210.6 (C9), 197.8 (C7), 140.4 (C5), 135.8, 135.6, 129.9, 127.8 (C-*C*H of phenyl), 132.9, 132.6 (*C*-CH of phenyl), 133.1 (C6), 97.2 (C1), 82.1 (C4), 65.7 (*C*H_2-O), 54.9 (C8), 51.5 (C10), 26.8 [C-(*C*H_3)$_3$], 19.3 [*C*-(CH_3)$_3$], 24.1, 20.8, 19.1, 15.1 (5 × *C*H_3) ppm. $C_{30}H_{38}SiO_6$ (522.7): calcd. C 68.93, H 7.33, O 18.36; found C 68.74, H 7.29. IR (KBr): ṽ = 3525 (O−H), 1690 (C=O), 1635 (C=O), 1113 (Si−O), 824 (O−O) cm^{-1}. MS (DCI /NH_3): *m*/*z* (%) = 540 [MNH_4]$^+$ (69), 344 (24), 330 (100).

4-(*tert*-Butyldiphenylsilyloxymethyl)-1-hydroxy-4,8,8,10,10-pentamethyl-2,3-dioxabicyclo[4.4.0]dec-5-ene-7,9-dione (15b): ^{1}H NMR (400 MHz, $CDCl_3$): δ = 7.57−7.61 (m, 4 H, Ar), 7.39−7.41 (m, 6 H, Ar), 7.12 (s, 1 H, =C*H*), 3.72, 3.65 (AB system, J_{AB} = 11.32 Hz, 2 H, CH_2OSi), 1.36, 1.35, 1.33, 1.31, 1.02 (5s, 15 H, 5 × CH_3), 0.97 [s, 9 H, C(CH_3)$_3$] ppm. ^{13}C NMR (100.64 MHz, $CDCl_3$) δ = 210.6 (C9), 197. 7 (C7), 140.4 (C5), 135.8; 135.6, 130.3, 130.2, 128.5, 128.2 (C-*C*H of phenyl), 132.5, 132.3 (*C*-CH of phenyl), 134.1 (C6), 97.5 (C1), 83.5 (C4), 67.2 (C16), 55.2 (C8), 51.4 (C10), 26.9 [C(*C*H_3)$_3$], 26.7 (C14), 23.8 (C13), 20.7 (C11), 19.4 (C15), 19.3 [*C*(CH_3)$_3$], 15.3 (C12) ppm. IR (neat): ṽ = 3541 (O−H), 1688 (C=O), 1637 (C=O), 1109 (Si−O), 823 (O−O) cm^{-1}. MS (DCI /NH_3): *m*/*z* (%) = 540 [MNH_4]$^+$ (100), 523 [M +1]$^+$ (4), 522 [M] (9).

1-Methoxy-4,4,8,8,10,10-hexamethyl-2,3-dioxabicyclo[4.4.0]dec-5-ene-7,9-dione (16): *n*BuLi (82 μL, 0.13 mmol) was added slowly, under argon at −78 °C, to a stirred solution of **13** (35 mg, 0.13 mmol) in THF (3 mL), and the mixture was allowed to warm up to −20 °C. After 15 min, TfOMe (24.6 mg, 0.15 mmol) was added at −20 °C. The reaction mixture was stirred for 30 min and was then extracted with diethyl ether. The extract was dried ($MgSO_4$) and concentrated to give **16** as an oil. Purification by silica gel chromatography (eluent petroleum ether/ethyl acetate, 9:1) gave **16** (26 mg, 70%). ^{1}H NMR (250 MHz, $CDCl_3$): δ = 7.35 (s, 1 H, C-C*H*), 3.44 (s, 3 H, OCH_3), 1.45, 1.35, 1.32, 1.28, 1.27, 1.03 (6s, 18 H, 6 × CH_3) ppm. ^{13}C NMR (50 MHz, $CDCl_3$), δ = 210.5 (C9), 198.9 (C7), 145.7 (C5), 128.2 (C6), 100.3 (C1), 78.8 (C4), 54.7 (O-*C*H_3), 53.1 (C10), 25.9, 24.7, 23.8, 23.5, 21.6, 15.8 (6 × CH_3) ppm. MS (DCI/NH_3): *m*/*z* (%) = 300 [MNH_4^+] (100), 283 [M +1]$^+$ (13), 210 (67).

1-Methoxy-4,8,8,10,10-pentamethyl-4-phenyl-2,3-dioxabicyclo-[4.4.0]dec-5-ene-7,9-dione (17a): Same procedure as for **16**; yield 80%. ^{1}H NMR (250 MHz, $CDCl_3$): δ = 7.67 (s, 1 H, C=C*H*), 7.30 (m, 5 H, Ar), 3.53 (s, 3 H, OCH_3), 1.61 [s, 3 H, CH-*C*H_3(Ph)], 1.33, 1.32, 1.17, 0.60 (4s, 12 H, 4 × CH_3) ppm. ^{13}C NMR (50 MHz, $CDCl_3$): δ = 210.5 (C9), 199.3 (C7), 143.9 (C5), 141.9 (C6), 129.4, 128.4, 127.9, 125.4 (Ar), 100.3 (C1), 81.8 (C4), 54.8 (C8), 54.6 (O-*C*H_3), 53.4 (C10), 26.4, 26.1, 24.9, 21.1, 15.4 (5 × *C*H_3) ppm.

1-Methoxy-4,8,8,10,10-pentamethyl-4-phenyl-2,3-dioxabicyclo-[4.4.0]dec-5-ene-7,9-dione (17b): Same procedure as for **16**; yield 67%. ^{1}H NMR (250 MHz, $CDCl_3$): δ = 7.70 (s, 1 H, C=C*H*), 7.44 (m, 5 H, Ar,), 3.44 (s, 3 H, OCH_3), 1.85 [s, 3 H, CH-*C*H_3(Ph)], 1.37, 1.34, 1.31, 1.15 (4s, 12 H, 4 × CH_3) ppm. ^{13}C NMR (50 MHz, $CDCl_3$): δ = 210.7 (C9), 198.6 (C7), 145.1 (C5), 138.2 (C6), 128.6, 129.1, 129.0, 126.2, 125.4 (Ar), 100.9 (C1), 81.9 (C4), 54.9 (C8), 53.5 (C10), 54.9 (O-*C*H_3), 26.0, 24.8, 23.7, 21.7, 15.6 (5 × *C*H_3) ppm. MS (DCI/NH_3): *m*/*z* (%) = 362 [MNH_4]$^+$ (46), 313 (100), 330 (21).

4-(*tert*-Butyldiphenylsilyloxymethyl)-1-methoxy-4,8,8,10,10-pentamethyl-2,3-dioxabicyclo[4.4.0]dec-5-ene-7,9-dione (18a): Same procedure as for **16**, yield 71%. ^{1}H NMR (400 MHz, $CDCl_3$) : δ = 7.67−7.59 (m, 4 H, Ar), 7.40 (s, 1 H, =C*H*), 7.39−7.32 (m, 6 H, Ar) 3.77, 3.67 (AB system, J_{AB} = 10.2 Hz, 2 H, CH_2OSi), 3.43 (s, 3 H, CH_3O), 1.47 1.27 1.24 1.19 (4s, 4 × CH_3), 1.06 [s, 9 H, C(CH_3)$_3$], 0.60 (s, 3 H, CH_3) ppm. ^{13}C NMR (100.64 MHz, $CDCl_3$): δ = 210.5 (C9), 198.5 (C7), 143.2 (C5), 135.9, 135.7, 130.1, 128.0 (C-*C*H of phenyl), 132.7, 133.2 (*C*-CH of phenyl), 129.8 (C6), 100.3 (C1), 81.6 (C4), 65.7 (C16), 55.8 (C8), 55.0 (O*C*H_3), 53.7 (C10), 27.0 [C(*C*H_3)$_3$], 26.1 (C13), 24.9 (C14), 21.6 (C11), 19.5 [*C*(CH_3)$_3$], 19.1 (C15), 15.7 (C12) ppm. IR (neat): ṽ = 1691 (C=O), 1640 (C=O), 1108 (Si−O), 823 (O−O) cm^{-1}. MS (DCI /NH_3): *m*/*z* (%) = 540 [MNH_4]$^+$ (36), 522 [M] (2), 299 (100).

4-(*tert*-Butyldiphenylsilyloxymethyl)-1-methoxy-4,8,8,10,10-pentamethyl-2,3-dioxabicyclo[4.4.0]dec-5-ene-7,9-dione (18b): Same pro-

cedure as for **18a**; yield 74%. ^{1}H NMR (250 MHz, $CDCl_3$) : δ = 7.69−7.62 (m, 4 H, Ar), 7.47 (s, 1 H, =C*H*), 7.45−7.35 (m, 6 H, Ar), 3.71, 3.69 (AB system, J_{AB} = 11.1 Hz, 2 H, CH_2OSi), 3.41 (s, 3 H, OCH_3), 1.43, 1.36, 1.32, 1.30, 1.06 (5s, 5 × CH_3), 1.04 [s, 9 H, C(CH_3)$_3$] ppm. ^{13}C NMR (100.64 MHz, $CDCl_3$): δ = 210.6 (C9), 198.6 (C7), 143.7 (C5), 135.8, 135.7, 130.2, 130.1, 128.1, 128.0, (C-*C*H of phenyl), 132.6, 132.5 (*C*-CH of phenyl), 129.8 (C6), 100.7 (C1), 82.6 (C4), 67.2 (C16), 55.0 (C17), 54.9 (C8), 53.3 (C10), 26.9 [C(*C*H$_3$)$_3$], 26.1 (C14), 24.9 (C13), 20.8 (C11), 19.6 (C15), 19.3 [*C*(CH$_3$)$_3$], 15.7 (C12) ppm. IR (neat): $\tilde{\nu}$ = 1691 (C=O), 1638 (C=O), 1102 (Si−O), 819 (O−O) cm^{-1}. MS (DCI /NH_3): *m*/*z* (%) = 540 [MNH_4]$^+$ (100).

In vitro Antimalarial Activity: The Nigerian strain of *Plasmodium falciparum* was maintained in culture by the method of Trager and Jensen.[17] The activity of the compounds against the in vitro growth of *P. falciparum* was determined according to Desjardins et al.,[18] by use of [^{3}H]hypoxanthine incorporation as an assessment of parasite growth. Stock drug solutions were prepared in 100% dimethyl sulfoxide (DMSO) at concentration of 10−40 mM and were serially diluted to the appropriate concentration with complete medium. Assays were performed in sterile 96-well microtiter plates. The final volume in each well was 200 μL, consisting of 50 μL of complete medium (RPMI 1640 containing 25 mM HEPES-buffer, pH 7.4 and 10% AB$^+$ human serum) either without (controls) or with drug and 150 μL of *P. falciparum*-infected erythrocyte suspension (1.5% final hematocrit and 0.6% parasitemia). After 48 h incubation at 37 °C, 30 μL of complete medium containing 0.7 μCi [^{3}H]hypoxanthine were added to each well. After 18 h at 37 °C, the cells were lysed by use of an automatic cell harvester and the parasite macromolecules, including radioactive nucleic acids, were harvested onto glass fibre filters. The filters were counted for radioactivity in a liquid scintillation spectrometer. The radioactivity background was obtained from incubation of non-infected erythrocytes under the same conditions, and deducted. Each drug was tested in triplicate at least twice with different batches of cells and parasite growth was compared to that in control wells − representing 100% parasite growth. Parasitic viability was expressed as IC_{50}, which is the drug concentration causing 50% parasite growth inhibition.

Acknowledgments

We thank Christiane Vidal for molecular modelling assistance, and Sharon Wein and Marjorie Maynadier for drug testing. Financial support by the MESR and CNRS is gratefully acknowledged.

[1] B. B. Snider, Z. Shi, *J. Org. Chem.* **1990**, *55*, 5669−5671.
[2] [2a] W. Jefford, M. G. H. Vicente, Y. Jacquier, F. Favarger, J. Mareda, P. Millason-Schmidt, G. Brunner, V. Burger, *Helv. Chim. Acta* **1996**, *79*, 1475−1487. [2b] J. N. Cummings, P. Ploypradith, G. H. Posner, *Adv. In Pharmacol.* **1997**, *37*, 253. [2c] R. K. Haynes, S. Vonwiller, *Acc. Chem. Res.* **1997**, *30*, 73. [2d] A. Robert, B. Meunier, *Chem. Soc. Rev.* **1998**, *27*, 273−279.
[3] P. M. O'Neill, N. L. Searle, K. J. Raynes, J. L. Maggs, S. A. Ward, R. C. Storr, B. K. Park, G. H. Posner, *Tetrahedron Lett.* **1998**, *39*, 6065−6068.
[4] W. Hofeinz, H. Burgin, E. Gocke, R. Jacquet, R. Masciadri, S. Schmid, H. Stohler, H. Urwyler, *Trop. Med. Parasitol.* **1994**, *45*, 261.
[5] M. D. Bachi, E. E. Korshin, R. Hoos, A. Splizman, *J. Heterocyclic Chem.* **2000**, *37*, 639−646.
[6] [6a] W. Peters, B. L. Robinson, G. Tovey, J.-C. Rossier, C. W. Jefford, *Ann. Trop. Med. Parasitol.* **1993**, *87*, 1−7. [6b] C. W. Jefford, S. Kohmoto, D. Jaggi, G. Timari, J.-C. Rossier, M. Rudaz, O. Barbuzzi, D. Gérard, V. Berger, P. Kamalaprija, J. Mareda, G. Bernardinelli, I. Manzanares, C. J. Canfield, S. L. Fleck, B. L. Robinson, W. Peters, *Helv. Chim. Acta* **1995**, *78*, 647−662.
[7] G. H. Posner, H. O'Dowd, P. Ploypradith, J. N. Cumming, S. Xie, T. A. Shapiro, *J. Med. Chem.* **1998**, *41*, 2164−2167.
[8] [8a] A. Robert, Y. Coppel, B. Meunier, *Chem. Commun.* **2002**, 414−415. [8b] J. Cazelles, A. Robert, B. Meunier, *J. Org. Chem.* **1999**, *64*, 6776−6781.
[9] E. L. Ghisalberti, *Phytochemistry* **1996**, *41*, 7−22, and references cited herein.
[10] M. Gavrilan, C. André-Barrès, M. Baltas, T. Tzedakis, L. Gorrichon, *Tetrahedron Letters* **2001**, *42*, 2465−2468.
[11] [11a] M. S. Workentin, F. Maran, D. D. M. Wayner, *J. Am. Chem. Soc.* **1995**, *117*, 2120−2121. [11b] R. L. Donkers, M. S. Workentin, *J. Phys. Chem. B* **1998**, *102*, 4061−4063.
[12] Molecular mechanic calculations were carried out with the Insight II (release 98;0) program with use of the Discover 3 calculation mode (MSI, San Diego, USA). Consistence valence force fields (CVFF) were used. Energetically optimised conformations were determined by sampling structures during molecular dynamic simulations. They were run for 10 ps at 500 K by the NVT method, with a 1fs time step. From the energy/time curves, six to seven minima were chosen and minimised. The same iterative operations (dynamic simulations and minimisation) were undertaken on these minima until no energy variation occurred. For each minimisation rms < 0.001.
[13] B. B. Snider, Z. Shi, *J. Am. Chem. Soc.* **1992**, *114*, 1790−1800.
[14] A. L. Baumstark, P. C. Vasquez, Y.-X. Chen, *J. Org. Chem.* **1994**, *59*, 6692−6696.
[15] S. Antonello, M. Musumeci, D. D. M. Wayner, F. Maran, *J. Am. Chem. Soc.* **1997**, *119*, 9541−9549.
[16] F. Zhang, D. Gosser, S. R. Meshnick, *Biochemical Pharmacology* **1972**, *43*, 1805−1809.
[17] J. B. Jensen, W. Trager, *J. Parasitol.* **1977**, *63*, 883−886.
[18] R. E. Desjardins, C. J. Canfield, J. D. Haynes, J. D. Chulay, *Antimicrob. Agents Chemother.* **1979**, *16*, 710−718.

Received March 11, 2003

